HHS Public Access

Author manuscript

J Mol Biol. Author manuscript; available in PMC 2019 October 12.

Published in final edited form as:

J Mol Biol. 2018 October 12; 430(20): 3764–3773. doi:10.1016/j.jmb.2018.07.005.

De novo designed alpha-sheet peptides inhibit functional amyloid formation of Streptococcus mutans biofilms

Natasha Paranjapye[a] and **Valerie Daggett**[a,b]

[a]Department of Bioengineering, Box 355013, University of Washington, Seattle, Washington, 98195-5013, United States of America

Abstract

Streptococcus mutans is a bacterial species that predominates in the oral microbiome. *S. mutans* binds to the tooth surface, metabolizes sugars and produces acid, leading to cavity formation. *S. mutans* can also cause infectious endocarditis. Recent evidence suggests that *S. mutans* biofilms contain amyloid fibrils. Amyloids are insoluble fibrillar protein aggregates, and bacteria use functional amyloids to improve robustness of their biofilms. While the functional amyloids in bacteria such as *E. coli* and *S. aureus* have been heavily investigated, little is known about the mechanism of *S. mutans* amyloid formation. Previous results from our lab with the amyloidogenic proteins and peptides from the aforementioned bacteria and other mammalian amyloid systems suggest that amyloid formation progresses via an intermediate that adopts a unique secondary structure – α-sheet. De novo designed peptides with alternating L- and D- amino acid also adopt an α–sheet secondary structure and inhibit amyloid formation by binding to soluble oligomeric species during amyloidogenesis. Inhibition of fibrillization by α-sheet peptides suggests the presence of α-sheet during amyloid formation. To investigate the mechanism of functional amyloid formation in *S. mutans*, α-sheet peptides were compared to Epigallocatechin gallate (EGCG) for their ability to inhibit fibril formation in *S. mutans*. Inhibition was demonstrated in a biofilm plate assay and on hydroxyapatite surfaces both in *S. mutans* alone and in bacteria from human saliva. The observed inhibition suggests that an α-sheet mediated mechanism may be operative during functional amyloid formation.

Graphical abstract

[b]Corresponding author. daggett@uw.edu.

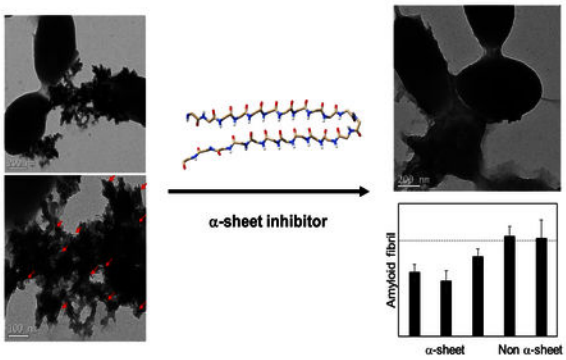

Keywords

α-sheet; *Streptococcus mutans*; functional amyloid; dental bacteria; peptide inhibitors

Introduction

Dental cavities are the second most prevalent human disease and account for 5–10% of public health expenditures in the industrialized world [1]. Cavities, also known as caries, will affect nearly 90% of young adults and 94% of adults within their lifetimes [2]. *Streptococcus mutans* is a gram-positive bacterial species that dominates in the oral microbiome and is the primary contributor to cavity formation. *S. mutans* is an acidophile that binds to the salivary pellicle, a layer of glycoproteins that coats the tooth surface. After the initial adhesion, the bacteria form a biofilm called a dental plaque [3]. As the biofilm grows, *S. mutans* outcompetes commensal bacteria, accesses deeper tissues of the tooth, and dissolves the tooth structure, resulting in cavity formation. In addition to causing cavities, *S. mutans* is a cause of infectious endocarditis, an inflammation of the endocardium of the heart [4]. Therefore, preventing accumulation of *S. mutans* biofilms is key to improving oral and overall health.

Numerous bacterial species, including *Staphylococcus aureus*, and *Escherichia Coli,* use amyloid fibrils to increase robustness or adhesion of their biofilms [5]. Amyloid fibrils are a common quaternary structure in which proteins aggregate to form strong, β-sheet rich fibrils. Recent Thioflavin T (ThT) fluorescence, Congo-Red (CR) birefringence, and Transmission Electron Microscopy (TEM) imaging of multiple *S. mutans* biofilm-associated proteins including SMU_63C, Antigen A, and P1, suggest they are amyloidogenic [6,7]. However, previous work did little to characterize amyloid formation in *S. mutans* biofilms under physiologic conditions.

Thioflavin T, or ThT, fluoresces upon binding to β–sheet structures present in amyloid fibrils [8]. Inhibitors like the polyphenolic small molecule Epigallocatechin gallate (EGCG) decrease fluorescence of multiple amyloidogenic *S. mutans* biofilm associated proteins [6,7]. EGCG inhibits amyloid fibril formation in mammalian amyloid proteins Aα and α-synuclein by binding to monomeric proteins and inducing formation of restructured oligomers that no longer form amyloid fibrils [9.10] It has also been suggested that EGCG

can remodel fibril structures. However, there have been no studies determining the mechanism of amyloid fibrillization in *S. mutans* and the mechanism by which EGCG inhibits *S. mutans* amyloid formation is unknown.

Atomistic molecular dynamics simulations have identified a unique secondary structure present as an intermediate during amyloidogenesis, called α-sheet [11]. α-sheet structure is characterized by alignment of backbone carbonyl groups on one side of the strand and the backbone amide groups on the other, which leads to a net molecular dipole. To test whether this nonstandard structure actually exists outside of the computer, we designed *de novo* alternating L- and D- amino acid hairpin peptides *in silico* with alternating chirality with residues with high propensity for the predicted structure [12]. Peptides with this structure inhibit fibril formation when incubated with amyloid-forming proteins in solution independent of sequence [12,13]. The arrangement of the main-chain atoms in an α-sheet is complementary to that observed in the molecular dynamics simulations. These synthetic α–sheet peptides inhibit fibril formation of different unrelated amyloidogenic proteins by preferentially binding to α-sheet-containing toxic oligomers along the path to amyloid [12,13,14], suggesting that binding and inhibition by α-sheet peptides reflects the presence of α-sheet during amyloid formation.

α-sheet peptides inhibit amyloid formation in both mammalian and bacterial systems. Notably, α-sheet peptides have been shown recently to inhibit functional amyloid formation in *S. aureus* biofilms [15]. The *S. aureus* functional amyloid system has been well-characterized, and α-sheet peptides decrease amyloid formation of the protein PSMα−1, which is the primary component of *S. aureus* biofilm amyloids, by selective binding to the soluble oligomers. Therefore, α–sheet peptides are attractive as potential inhibitors of functional amyloid formation in *S. mutans.* The mechanism of functional amyloid formation in *S. mutans* is not yet understood, and their biofilms have not been studied as a function of time at physiological temperatures. The exact proteins that constitute *S. mutans* amyloid fibrils are also not currently known. However, comparisons between the behavior of *S. aureus* and *S. mutans* in the presence of α-sheet inhibitors may reveal similarities or differences in the mechanism of fibril formation. The effectiveness of α-sheet peptides against *S. mutans* biofilms would suggest that an α–sheet intermediate is present in the pathway to functional amyloid formation. Therefore, evaluating the effectiveness of these peptides provides useful information about the time-dependent aggregation behavior of proteins in *S. mutans* biofilms. α-sheet peptides include a common hairpin turn sequence, arginine-glycine endcaps to aid in solubility, and variable regions that have been manipulated to create a library of α–sheet inhibitors. Herein, three α-sheet peptides- AP90, disulfide-bridged AP407, and dimerized AP193- were compared to random coil and β-hairpin controls for their ability to inhibit amyloid formation in *S. mutans* biofilms and in bacteria present in whole human saliva to shed light on the mechanism of amyloidogenesis and its role in biofilm formation and stability.

Results

Optimization of ThT biofilm assay

Thioflavin T (ThT) binds the cross-β structure present in amyloid fibrils [8]. To determine amyloid fibril content of *S. mutans* biofilms, a ThT-based plate assay was developed based on a protocol by Bleem *et. al.* (Figure 1) [15]. To establish the time-dependent fibril content of *S. mutans* biofilms, plates were grown for various time periods up to 48 hours (Figure 2). A plateau in the ThT fluorescence was seen around 24 hours, with the main increase in ThT fluorescence occurring during the 12 hour to 24 hour time period. Based on these results, a window of 24–28 hours of incubation was chosen for inhibition studies to maximize biofilm maturity and the fibril content.

To determine the ability of the ThT plate assay to detect amyloid fibril inhibition in *S. mutans*, a dose-response curve was obtained with EGCG, a known amyloid inhibitor across multiple systems (Figure 3) [10]. The assay detected significant decreases in ThT fluorescence with increasing concentration of EGCG ($p < 0.05$) at concentrations of 50 μM EGCG and greater. There was up to a 73% decrease in ThT fluorescence with 500 μM EGCG ($p = 0.001$).

Screening of peptides with ThT plate assay

The peptides AP90, AP407, AP193, P411, and P1 were screened for their ability to inhibit amyloid fibril formation using the optimized ThT plate assay. Sequences of these peptides are provided in Table 1. α-sheet peptides, with the AP nomenclature, AP90 (previously called α1 by Hopping *et. al.* 2014), AP407, and AP193 show unique structural characteristics indicative of α-sheet secondary structure, including a featureless structure by circular dicroism (CD) due to cancellation of signal by the alternating chirality of amino acids [12]. AP407 is an α-sheet peptide based on AP90 with a disulfide linkage between C7 and C16 (formerly S7 and M16 in AP90). AP193 differs in sequence from AP90 and is dimerized via C19. The β-sheet hairpin P411 was used as a β-sheet conformational control, and the random coil peptide P1 was used as a unstructured peptide control.

Peptides with various secondary structures were tested for their ability to inhibit amyloid formation in biofilms using the ThT plate assay (Figure 4). These peptides do not bind ThT, such that ThT fluorescence reflects the amount of fibrils present [12,15]. The AP193 dimer at 40 μM decreased ThT fluorescence by 33% ($p = 0.007$). A 42% decrease in ThT fluorescence compared to the control was seen with 85 μM AP407, the disulfide-bridged α-sheet peptide ($p < 0.0001$). AP90, an α-sheet peptide without the disulfide linkage in AP407, caused a 16% decrease in ThT fluorescence at 85 μM ($p = 0.017$). However, the β-sheet hairpin control P411 and the random coil control P1 had no significant effect.

TEM biofilm imaging

To determine the effect of adding peptide inhibitors to biofilms, whole biofilms were grown in plates, rinsed, and imaged with no peptide, and with addition of peptide inhibitors AP90 (100 μM) or AP193 dimer (50 μM) using TEM (Figure 5). Distinct fibrillar structures were found in the extracellular material surrounding cells with no peptide present, but such

structures were not observed around cells when α-sheet peptide was present. One region of fibrillar extracellular material was seen with addition of 100 μM AP90, but it was not heavily attached to cells as seen in the condition with no peptide. No regions of fibrillar structures were found in biofilms with 50 uM AP193. These results correspond to results seen in the ThT plate assay, where AP193 inhibited more strongly than AP90.

S. mutans and salivary bacteria binding to hydroxyapatite surfaces

To assess inhibition of amyloid fibrils in *S. mutans* adhered to tooth-like surfaces, *S. mutans* was grown on ceramic-hydroxyapatite particles (Figure 6). Hydroxyapatite is the primary mineral present in the structure of a tooth, so this assay is a more physiologically relevant model of *S. mutans* accumulation [16]. ThT fluorescence of adhered cells was determined after 24 hours of growth. The hydroxyapatite binding was again optimized by obtaining a dose-response curve of EGCG, which shows a similar dose-dependent reduction in ThT fluorescence to *S. mutans* biofilms grown in plates (Figure 7). 250 μM EGCG resulted in a 52% reduction in ThT fluorescence, compared to the 53% reduction in ThT fluorescence seen in the plate assay with the same concentration (Figure 3). Peptides were added to medium and hydroxyapatite ceramic particles prior to cell growth. Addition of AP90 (100 μM) led to a 20% decrease in ThT fluorescence, comparable to decreases seen in the plate assay. Both AP193 monomer and dimer caused significant decreases in ThT fluorescence (23% and 63% respectively) of *S. mutans* adhered to hydroxyapatite resin (Figure 8).

To better replicate the biological conditions for biofilm on teeth, artificial salivary pellicles with associated bacteria were formed using whole human saliva. The bacteria adhered to these salivary pellicles were grown on hydroxyapatite-ceramic resin. After 24 hours of growth, ThT fluorescence of cells grown on the hydroxyapatite-ceramic resin was read. With the addition of α-sheet peptides, there was a significant decrease in ThT fluorescence compared to saliva grown with media and vehicle only for all 5 donors (Figure 9). A broad range of inhibition was observed, from 83% inhibition in subject 1, to 27% inhibition in subject 3. Despite the variable growth of bacteria in saliva from different subjects, ThT fluorescence of each sample decreased with addition of α-sheet peptide.

Discussion

The binding of a conformation-specific antibody to multiple amyloidogenic proteins in the nucleation phases of amyloid formation suggests a shared nonstandard secondary structure on the pathway to amyloid fibril formation [17]. Nuclear magnetic resonance (NMR), Fourier-transform infrared spectrometry (FTIR), and circular dichroism (CD) results indicate a lack of α-helical or β-sheet secondary structure in the lag phase of amyloid formation in the amyloid β-peptide (Aβ), which is implicated in Alzheimer's disease [18,19,20]. A similar lack of defined structure in the nucleation phase of amyloid formation of the islet amyloid polypeptide (IAPP) has been demonstrated by CD [21,22].

The behavior of multiple amyloidogenic proteins in the presence of α-sheet inhibitors has been studied in depth. Several α-sheet peptide designs inhibit aggregation of Aβ up to 96%, as indicated by ThT binding [20]. ThT binding also demonstrates up to 83% inhibition of amyloid formation of islet amyloid polypeptide (IAPP) and 81% inhibition of ThT

fluorescence of transthyretin with an excess of α-sheet peptides [12,13]. Inhibition occurs via binding of α-sheet peptides to soluble oligomers that share the α-sheet structure [20,21]. These results suggest that the common structural motif present in these well-characterized amyloid diseases is α-sheet. Moreover, there appears to be a mix of α-sheet and β-sheet in fibrils comprised of a transthyretin-derived peptide [23].

Similar inhibition of ThT fluorescence and amyloid formation was recently demonstrated by Bleem *et. al.* in the functional amyloid formation of phenol soluble modulins (PSM) in *S. aureus* biofilms [15]. PSMα−1 adopts a featureless CD spectrum in the nucleation phase of amyloid formation similar to the mammalian amyloid proteins, transitioning from α-helical structure, to α-sheet, to β-sheet. Because the dominant peptide responsible for amyloid formation is known, Bleem *et. al.* also tracked inhibition of PSMα1 incubated with AP90 over time, with preferential binding of PSMα1 to AP90 occurring in the α-sheet-rich phase versus the β-sheet fibrillar or α-helical phases. These results provide support for a common intermediate structure in the soluble oligomer species during amyloid formation in *S. aureus* and the previously described mammalian systems.

Here, we demonstrate comparable results in *S. mutans,* which suggests that a similar mechanism of amyloid fibrillization is operative in this unrelated pathogen. AP90 and AP407 inhibit ThT fluorescence in *S. aureus* biofilms and *S. mutans*. Unlike the ThT biofilm assay used in *S. aureus, S. mutans* biofilms were resuspended in the ThT solution itself rather than in PBS because of high variability when resuspending in PBS. Unfortunately, however, this change leads to higher background fluorescence and a lower percentage inhibition. Nevertheless, as with *S. aureus*, the effects are more striking by TEM where nearly complete inhibition of amyloid fibril structures surrounding cells is observed upon addition of α-sheet compound. The decreases in fibrillar content correspond to inhibition quantified by ThT fluorescence. These correlations suggest that *S. mutans* may share an intermediate α-sheet structured species in the pathway to amyloid formation, however, the proposed presence of α-sheet is necessarily indirect based on the preference of the different inhibitors tested until the pure components of the system are characterized structurally.

The hydroxyapatite-binding assay demonstrates that fibril inhibition of *S. mutans* and oral bacterial accumulations by α-sheet peptides in a more biologically relevant setting. Dental plaque contains multiple bacterial species, so studying the effects of α-sheet inhibitors on heterogenous accumulations is key to understanding the role of amyloid fibrils in dental plaque [24]. The ability of α-sheet peptides to inhibit amyloid fibril formation in bacteria grown from five separate human saliva samples suggests a broad role of the α-sheet mechanism in oral bacterial accumulations.

Currently, very little is known about functional amyloid fibrils in *S. mutans* biofilms. Multiple possible biofilm-associated proteins could potentially be responsible for amyloid fibril formation [7]. As the exact protein responsible for fibril formation in *S. mutans* has not been identified, amyloid fibrils were studied here in whole live bacteria in two different biologically relevant environments. Once the protein or peptide responsible for amyloid formation has been identified, the isolated pure protein can be characterized by performing ThT assays with α-sheet inhibitors and conformational controls, as well as CD of the

isolated protein over time to confirm the presence of an α-sheet intermediate. Here, we present the first TEM images of fibril-like extracellular material surrounding cells in whole *S. mutans* biofilms. We demonstrate inhibition of amyloid formation in live bacteria, along with visual decreases in extracellular fibrillar material with TEM imaging. The correlations between the behavior of different amyloid proteins in the presence of α-sheet peptide inhibitors suggest that a similar intermediate with α-sheet secondary structure is present on the amyloid fibril formation pathway of *S. mutans.* These results present the opportunity for novel therapies to disrupt accumulation of *S. mutans* on the tooth surface using α-sheet inhibitors, ultimately preventing the pathogen from giving rise to cavities or further systemic infections.

Materials and Methods

α-sheet Peptide Synthesis

The peptides used herein are described in Table 1. Peptides were synthesized using Fmoc solid-phase peptide synthesis, purified using high-performance liquid chromatography (HPLC), lyophilized, and stored at −20°C prior to use. Purified peptides were characterized using an ion-trap mass spectrometer to verify their identity. Detailed description of synthesis procedures used are included in Maris *et. al.* (2018) [14].

ThT Plate Assay

A ThT plate assay was used to monitor amyloid fibril formation using a protocol modified from Bleem *et. al.* (2017) (Figure 1) [15]. *Streptococcus mutans* UA159 [UAB577] was acquired from ATCC, originally isolated from a child with active caries (1982). Overnight cultures were grown in BHI medium with 30 mM sucrose at 37°C. These samples were then centrifuged and resuspended in BHI medium with 30 mM sucrose and 1% (v/v) EC Oxyrase$^{(R)}$ to ensure an oxygen-limited environment. The cultures were diluted to a final Optical Density at 600 nm (OD600) of 0.1 in the wells. These cultures were then mixed with inhibitors in water, or only water for blank conditions. AP193 was dimerized by dissolving in 1.5% (v/v) DMSO in CO_3^{2-} buffer (pH 9.6) and incubating at 37°C for 2 hours. The control biofilms had an equal volume of DMSO (1.5% v/v) in carbonate buffer added. Bacterial samples were aliquoted in quadruplicate in a clear 96-well plate. The plates were covered and sealed with parafilm three times before incubating statically at 37°C. ThT fluorescence was evaluated as a function of time to track amyloid growth, and for 28 hours during inhibition studies. Media and planktonic cells were gently removed using a vacuum, the adherent biofilms were rinsed with PBS (BupH, ThermoFisher Scientific). Thioflavin T (ThT) (Sigma-Aldrich) in PBS was then added to the wells for a final concentration of 22 μM and incubated statically at room temperature in the dark for 4 hours. The solution was pipetted up and down vigorously to resuspend the biofilms into solution. The plate was shaken at high speed for 30 seconds, sonicated for 30 seconds to detach and resuspend remaining biofilm. Samples were transferred to a black-walled 96 well plate. ThT fluorescence was measured using an excitation of 438 nm and emission of 495 nm (Perkin-Elmer Enspire plate reader).

Biofilm Transmission Electron Microscopy (TEM) Imaging

Biofilm samples were grown as described above with and without addition of peptide inhibitor in 1.5% DMSO (v/v) in carbonate buffer to a final well concentration of 100 μM (AP90), 50 μM (AP193 dimer, dimerized as above). The condition without peptide had an equal volume of 1.5% DMSO in carbonate buffer added. Biofilms were then rinsed with PBS and scraped from the wells of the plate into water and spotted onto formvar-coated copper grids. Samples were stained with 2% uranyl acetate for 2 minutes, dried under vacuum, and imaged using a FEI-Tecnai scanning transmission electron microscope (S/TEM).

Hydroxyapatite Binding Assay

CHT™ ceramic hydroxyapatite type I resin (20 μm) (Bio-Rad) was suspended in PBS and equally distributed to wells of a 96-well plate. To add *S. mutans* to hydroxyapatite, the PBS was removed by pipetting, and OD600 = 0.1 *S. mutans* cells in BHI with 30 mM sucrose and 1% (v/v) oxyrase were added to wells, with either buffer only or inhibitor in buffer. AP90 was dissolved in PBS (BupH, ThermoFisher Scientific) and AP193 was dissolved in 1.5% DMSO in carbonate buffer (pH 9.6). Plates were parafilmed three times and incubated statically for 24 hours at 37°C. After growth, planktonic cells and media were separated from hydroxyapatite-ceramic resin. PBS was added to plate wells, samples were pipetted to resuspend hydroxyapatite in liquid, and the suspension was transferred to tubes. PBS was removed, 22 μM ThT in PBS was added and the resin was agitated by vortexing 1 minute, then sonicating 1 minute to displace adhered cells from the resin into supernatant. The ThT supernatant was plated in triplicate in a clear bottomed, black-walled 364-well plate and measured using an excitation of 438 nm and emission of 495 nm (Perkin-Elmer Enspire plate reader).

Whole Human Saliva Sample Hydroxyapatite Binding

Whole human saliva was obtained from volunteer donors. Donors were instructed to brush teeth and not eat for 1 hour prior to collection time. Donors rinsed their mouth with distilled water for 1 minute, then collected approximately 5 mL saliva in a sterile falcon tube. Samples were stored on ice for no more than 2 hours prior to use. Saliva samples were centrifuged at 1500 rpm for 5 minutes, then added to hydroxyapatite resin in 96-well plates. Saliva was incubated with resin for 2 hours to allow the salivary pellicle to form and bacteria to adhere. Saliva was removed by pipetting and the resin was rinsed with PBS. BHI media with 30 mM sucrose and 1% (v/v) EC Oxyrase$^{(R)}$ was added to resin and allowed to incubate 24 hours at 37°C before transferring, rinsing and adding ThT, as described above.

Acknowledgments:

We thank Andee Ott for experimental contributions and assistance, Alissa Bleem for assistance with troubleshooting and initial characterization, Dr. James Bryers for use of lab space, Robyn Francisco for assistance with lab equipment and maintenance, Wai Pang Chan and Ellen Lavoie at the University of Washington Biology Imaging Facility and Molecular Analysis Facility (MAF) for assistance with TEM imaging, and Timothy Bi, Steven Hsu, and Dylan Shea for assistance with peptide synthesis and characterization. We also thank the University of Washington Mary Gates Endowment, the Department of Bioengineering, and the Office of Research for financial support of this research, as well as the National Institutes of Health (GMS 95808).

References

[1]. Fejerskov O, Kidd E. Dental Caries: The disease and its clinical management. 2nd ed. Wiley-Blackwell, 2009.

[2]. Chen F, Wang D. Novel technologies for the prevention and treatment of dental caries: a patent survey. Expert opinion on therapeutic patents. 2010;20:681–94. [PubMed: 20230309]

[3]. Selwitz RH, Ismail AI, Pitts NB. Dental caries. The Lancet. 2007;369:51–9.

[4]. McGhie D, Hutchison JG, Nye F, Ball AP. Infective endocarditis caused by Streptococcus mutans. Br Heart J. 1977;39:456–8. [PubMed: 869980]

[5]. DePas WH, Chapman MR. Microbial manipulation of the amyloid fold. Res Microbiol. 2012;163:592–606. [PubMed: 23108148]

[6]. Oli MW, Otoo HN, Crowley PJ, Heim KP, Nascimento MM, Ramsook CB, et al. Functional amyloid formation by Streptococcus mutans. Microbiology. 2012;158:2903–16. [PubMed: 23082034]

[7]. Besingi RN, Wenderska IB, Senadheera DB, Cvitkovitch DG, Long JR, Wen ZT, et al. Functional Amyloids in Streptococcus mutans, their use as Targets of Biofilm Inhibition and Initial Characterization of SMU_63c. Microbiology. 2017;163:488–501. [PubMed: 28141493]

[8]. LeVine H Quantification of β-sheet amyloid fibril structures with thioflavin T. Methods in Enzymology. 1999;309:274–84. [PubMed: 10507030]

[9]. Bieschke J, Russ J, Friedrich RP, Ehrnhoefer DE, Wobst H, Neugebauer K, et al. EGCG remodels mature alpha-synuclein and amyloid-beta fibrils and reduces cellular toxicity. Proc Natl Acad Sci U S A. 2010;107:7710–5. [PubMed: 20385841]

[10]. Palhano FL, Lee J, Grimster NP, Kelly JW. Toward the Molecular Mechanism(s) by Which EGCG Treatment Remodels Mature Amyloid Fibrils. Journal of the American Chemical Society. 2013;135:7503–10. [PubMed: 23611538]

[11]. Daggett V Alpha-sheet: The toxic conformer in amyloid diseases? Acc Chem Res. 2006;39:594–602. [PubMed: 16981675]

[12]. Hopping G, Kellock J, Barnwal RP, Law P, Bryers J, Varani G, et al. Designed alpha-sheet peptides inhibit amyloid formation by targeting toxic oligomers. Elife. 2014;3:e01681. [PubMed: 25027691]

[13]. Kellock J, Hopping G, Caughey B, Daggett V. Peptides Composed of Alternating L- and D-Amino Acids Inhibit Amyloidogenesis in Three Distinct Amyloid Systems Independent of Sequence. Journal of Molecular Biology. 2016;428:2317–28. [PubMed: 27012425]

[14]. Maris NL, Shea D, Bleem A, Bryers JD, Daggett V. Chemical and Physical Variability in Structural Isomers of an L/D α-Sheet Peptide Designed To Inhibit Amyloidogenesis. Biochemistry. 2018;57:507–10. [PubMed: 29202245]

[15]. Bleem A, Francisco R, Bryers JD, Daggett V. Designed α-sheet peptides suppress amyloid formation in Staphylococcus aureus biofilms. NPJ Biofilms and Microbiomes. 2017;3:16. [PubMed: 28685098]

[16]. Oktar FN, Kesenci K, Piskin E. Characterization of Processed Tooth Hydroxyapatite for Potential Biomedical Implant Applications. Artificial Cells, Blood Substitutes, and Biotechnology. 1999;27:367–79.

[17]. Kayed R, Head E, Thompson JL, McIntire TM, Milton SC, Cotman CW, et al. Common Structure of Soluble Amyloid Oligomers Implies Common Mechanism of Pathogenesis. Science. 2003;300:486. [PubMed: 12702875]

[18]. Kim JR, Muresan A, Lee KY, Murphy RM. Urea modulation of beta-amyloid fibril growth: experimental studies and kinetic models. Protein Sci. 2004;13:2888–98. [PubMed: 15459334]

[19]. Ahmed M, Davis J, Aucoin D, Sato T, Ahuja S, Aimoto S, et al. Structural conversion of neurotoxic amyloid-beta(1–42) oligomers to fibrils. Nat Struct Mol Biol. 2010;17:561–7. [PubMed: 20383142]

[20]. Shea D, Hsu CC, Bi T, Paranjapye N, Childers M, Cochran J, Tomberlin CP, Wang Z, Paris D, Zonderman J, Varani G, Link C, Mullan M, Daggett V. α-sheet as a driver of aggregation and toxicity in Alzheimer's Disease. 2018, to be submitted shortly.

[21]. Kayed R, Bernhagen J, Greenfield N, Sweimeh K, Brunner H, Voelter W, et al. Conformational transitions of islet amyloid polypeptide (IAPP) in amyloid formation in vitro. J Mol Biol. 1999;287:781–96. [PubMed: 10191146]

[22]. Hsu C-C, Templin A, Shea D, Kahn SE, Daggett V. Novel α-sheet compounds inhibit aggregation and toxicity of islet amyloid polypeptide, 2018, to be submitted shortly.

[23]. Hilaire MR, Ding B, Mukherjee D, Chen J, Gai F. Possible existence of α-sheets in the amyloid fibrils formed by a TTR105–115 mutant. J. Amer Chem Soc 2018, 140:629–635. [PubMed: 29241000]

[24]. Komori R, Sato T, Takano-Yamamoto T, Takahashi N. Microbial composition of dental plaque microflora on first molars with orthodontic bands and brackets, and the acidogenic potential of these bacteria. Journal of Oral Biosciences. 2012;54:107–12.

Highlights

- *Streptococcus mutans* has recently been identified to form functional amyloid, but little is known about the mechanism of amyloid fibril formation. Comparing the effects of α-sheet peptides in *S. mutans* and other amyloid systems sheds light on the intermediates present during fibril formation.
- Multiple α-sheet peptides inhibit amyloid fibril formation in *S. mutans* biofilms, and in bacteria present in whole human saliva samples compared to β-sheet and random coil control peptides. Inhibition occurred in biofilms grown in a plate and in bacterial accumulations on tooth-like hydroxyapatite surfaces.
- TEM imaging reveals that fibril structures present in *S. mutans* biofilms are no longer present upon addition of α-sheet peptides.
- These results suggest that an α-sheet intermediate is involved in amyloid fibril formation in *S. mutans* biofilms.

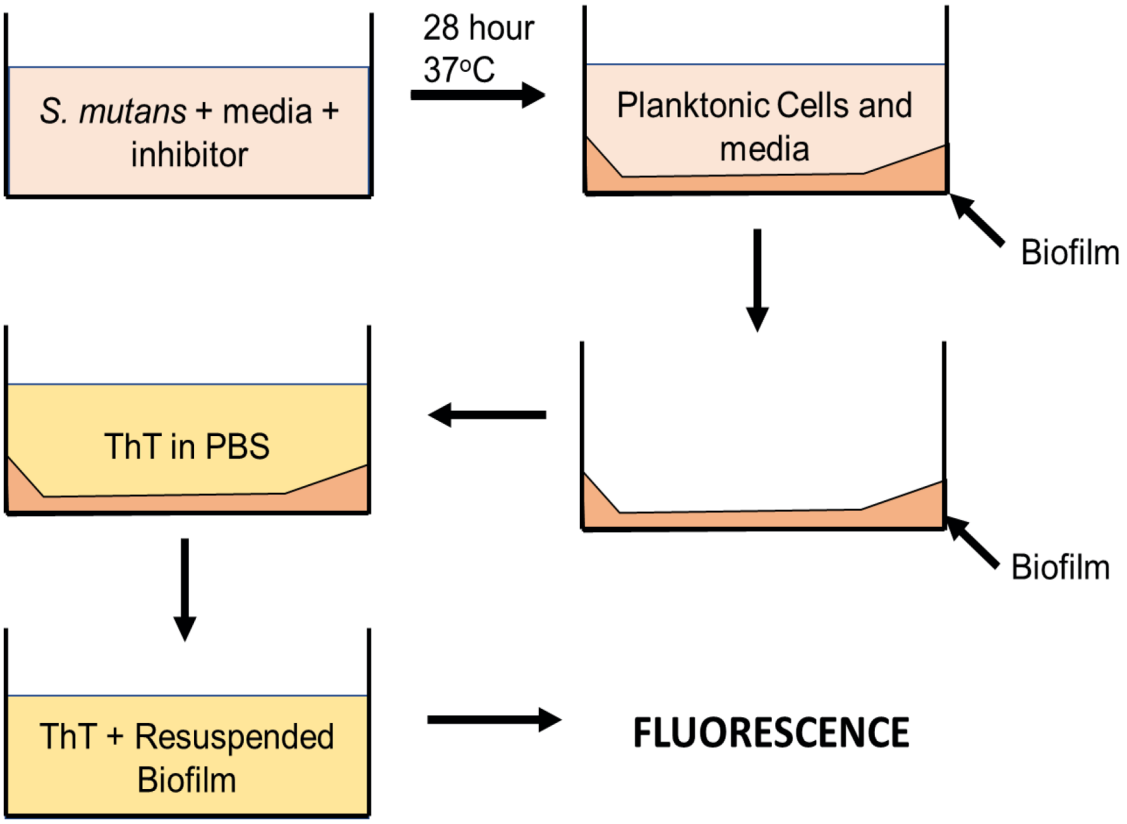

Figure 1.

Schematic of biofilm ThT plate assay. Bacteria is grown in media with either inhibitor or solvent alone in 96-wells until a biofilm forms on the bottom of the well. Planktonic cells and media are removed, ThT solution is added, and the biofilm is resuspended in the ThT solution. The fluorescence of the resuspended biofilm in ThT indicates quantifies the relative amount of fibril content in the biofilms.

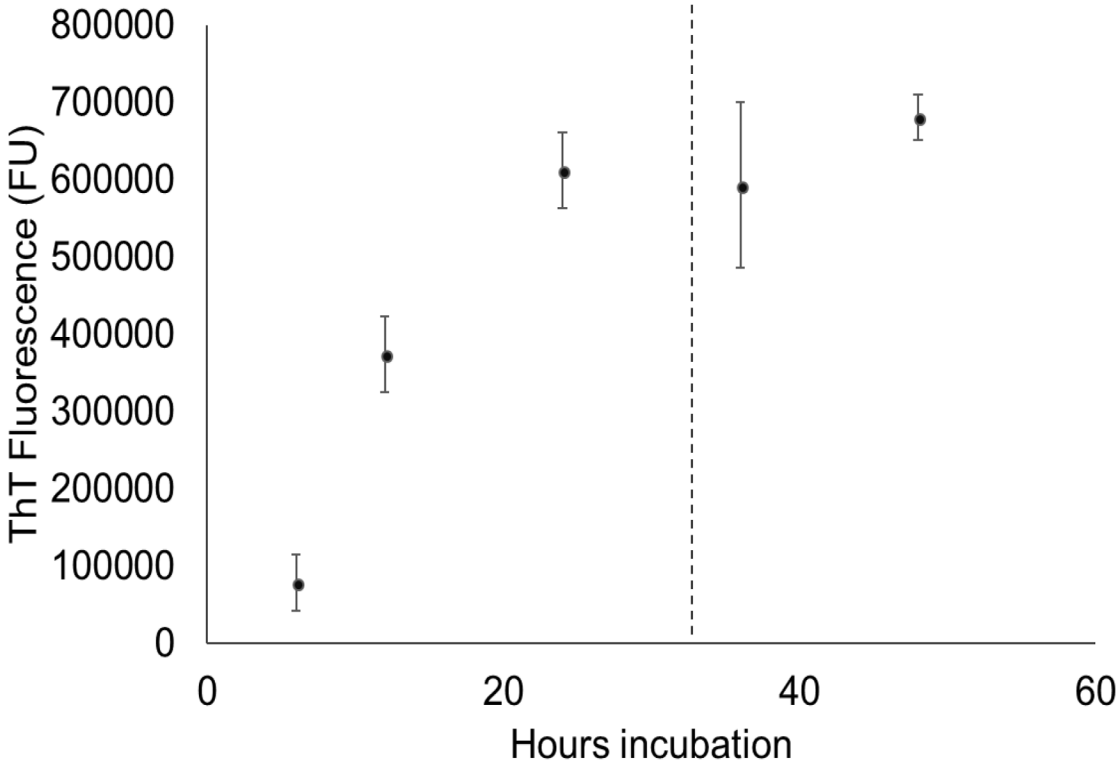

Figure 2.

Time-course of ThT fluorescence for biofilms grown in the biofilm ThT plate assay. Biofilms were grown in 96-well plates and fluorescence was read at timepoints up to 48 hours. A plateau in ThT fluorescence was seen around t = 24 hours. The fluorescence was quantified according to the protocol in Figure 1.

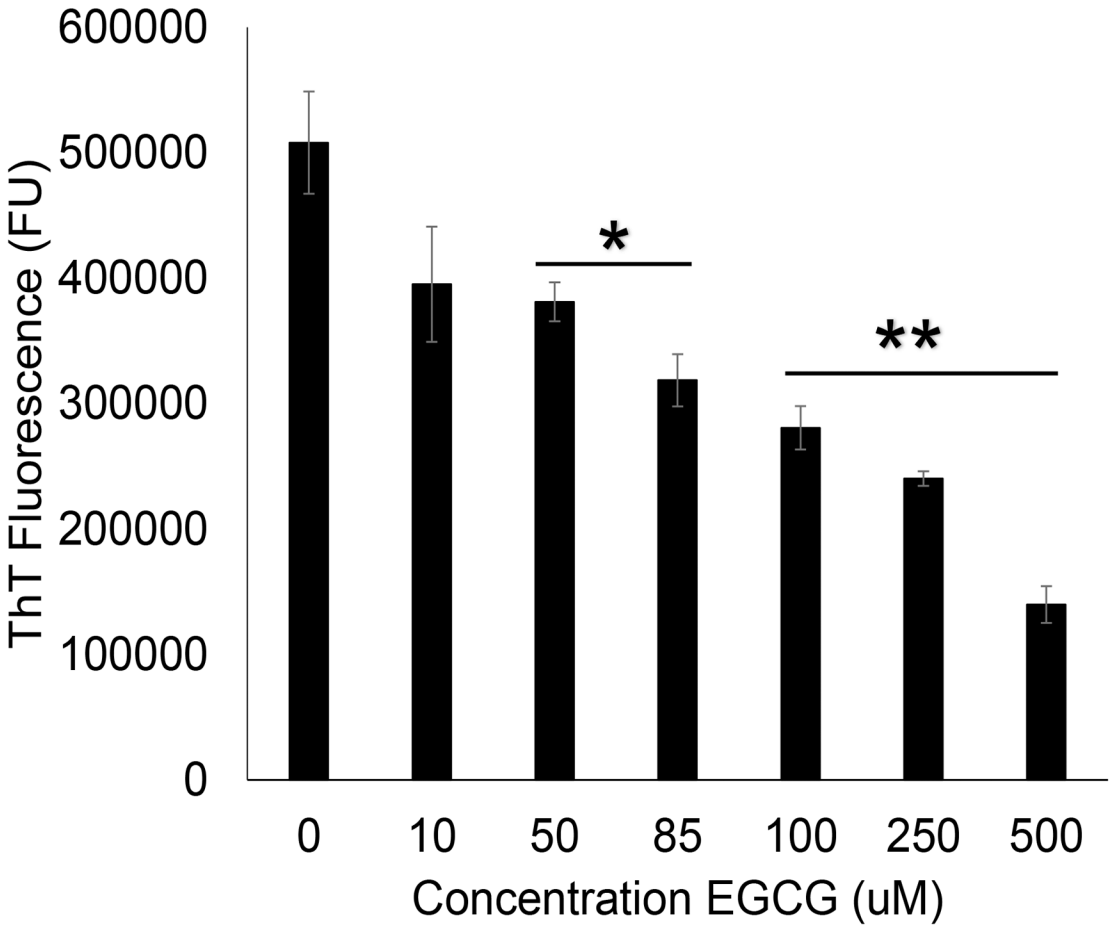

Figure 3.

ThT fluorescence of *S. mutans* biofilms in plate assay with addition of EGCG in PBS. There was a dose-dependent reduction in ThT fluorescence with increasing EGCG concentration, up to a 73% reduction in ThT fluorescence at 500 μM EGCG. (* = $p < 0.05$, ** = $p < 0.01$, compared to 0 μM EGCG)

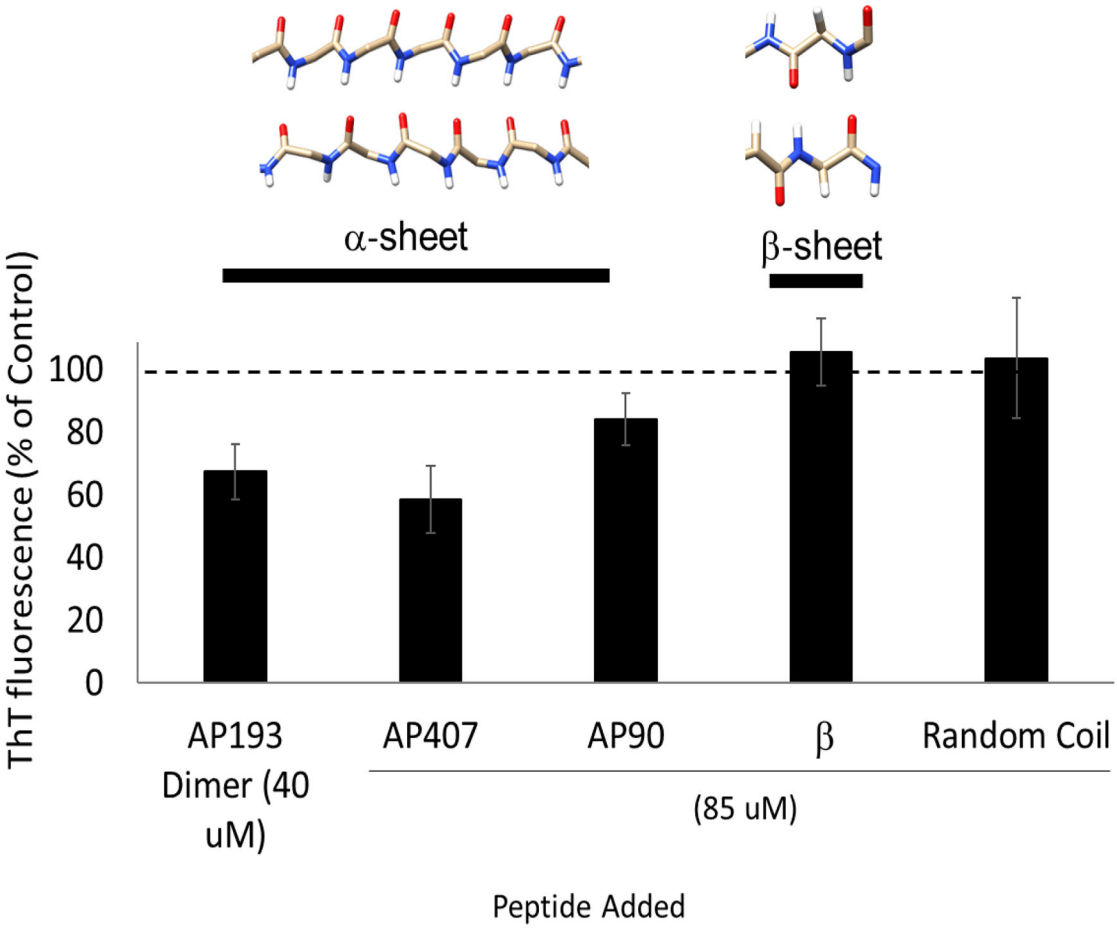

Figure 4.

ThT Fluorescence of *S. mutans* with addition of α-sheet peptides 40 μM AP193 (dimerized) compared to biofilms with only 1.5% DMSO in CO_3^{2-} added, which causes a 33% ($p = 0.007$) decrease in ThT fluorescence. 85 μM AP407 caused a 42% decrease in ThT fluorescence ($p < 0.0001$) and AP90 caused a 16% reduction in ThT fluorescence ($p = 0.02$) compared to controls with only water. However, the beta sheet and random coil control peptides showed no significant decrease in ThT fluorescence.

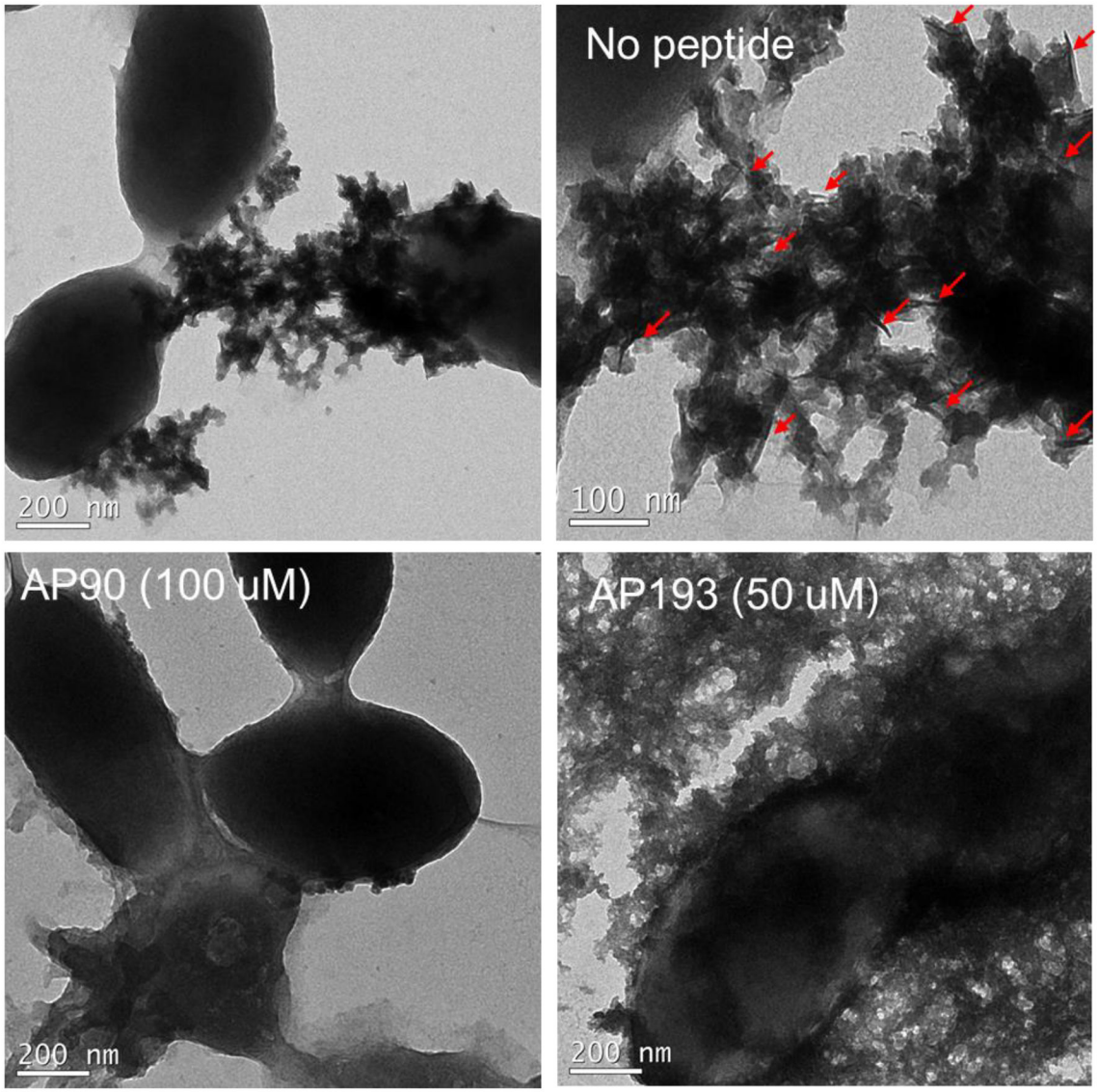

Figure 5.

Transmission electron microscopy (TEM) imaging of biofilms with vehicle only and no peptide (5A), 100 μM AP90 in 1.5% DMSO in carbonate buffer (5B) and 50 μM AP193 dimer in 1.5% DMSO in carbonate buffer. Addition of α-sheet peptides led to almost no fibrillar material being visible outside of cells, compared to significant fibrillar material outside of cells without peptide added.

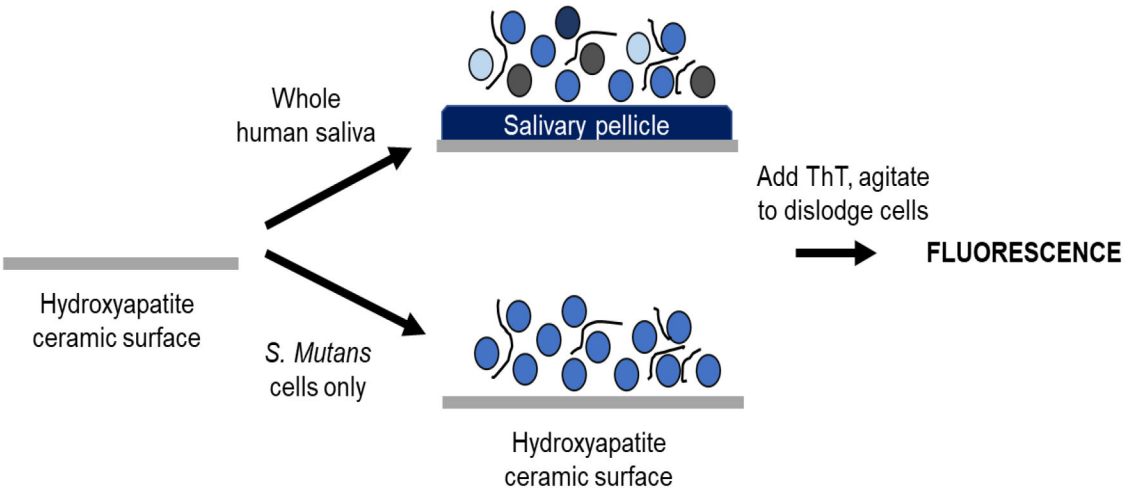

Figure 6.

Schematic of procedure for hydroxyapatite binding assay. For saliva studies, hydroxyapatite-ceramic particles were incubated with saliva to form an artificial salivary pellicle with associated bacteria. Media was then added and samples were grown 24 hours prior to staining with ThT. For *S. mutans* only studies, *S. mutans* in media was added directly to hydroxyapatite ceramic particles and grown 24 hours prior to ThT staining.

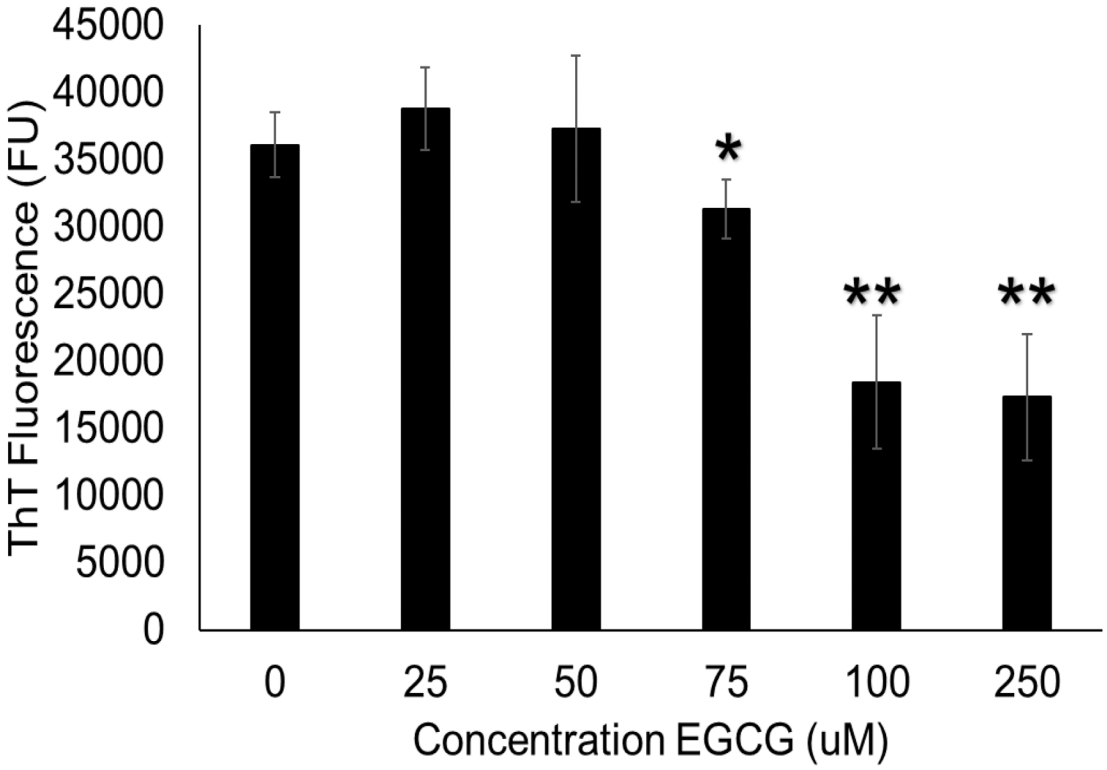

Figure 7.

EGCG dose response for hydroxyapatite binding assay with *S. mutans* in media alone (no saliva), there was a dose dependent decrease in ThT fluorescence with addition of EGCG, a 53% decrease in ThT fluorescence was seen with 250 μM EGCG, comparable to the decrease seen in the plate assay. (* = $p < 0.05$, ** = $p < 0.01$, compared to 0 μM EGCG)

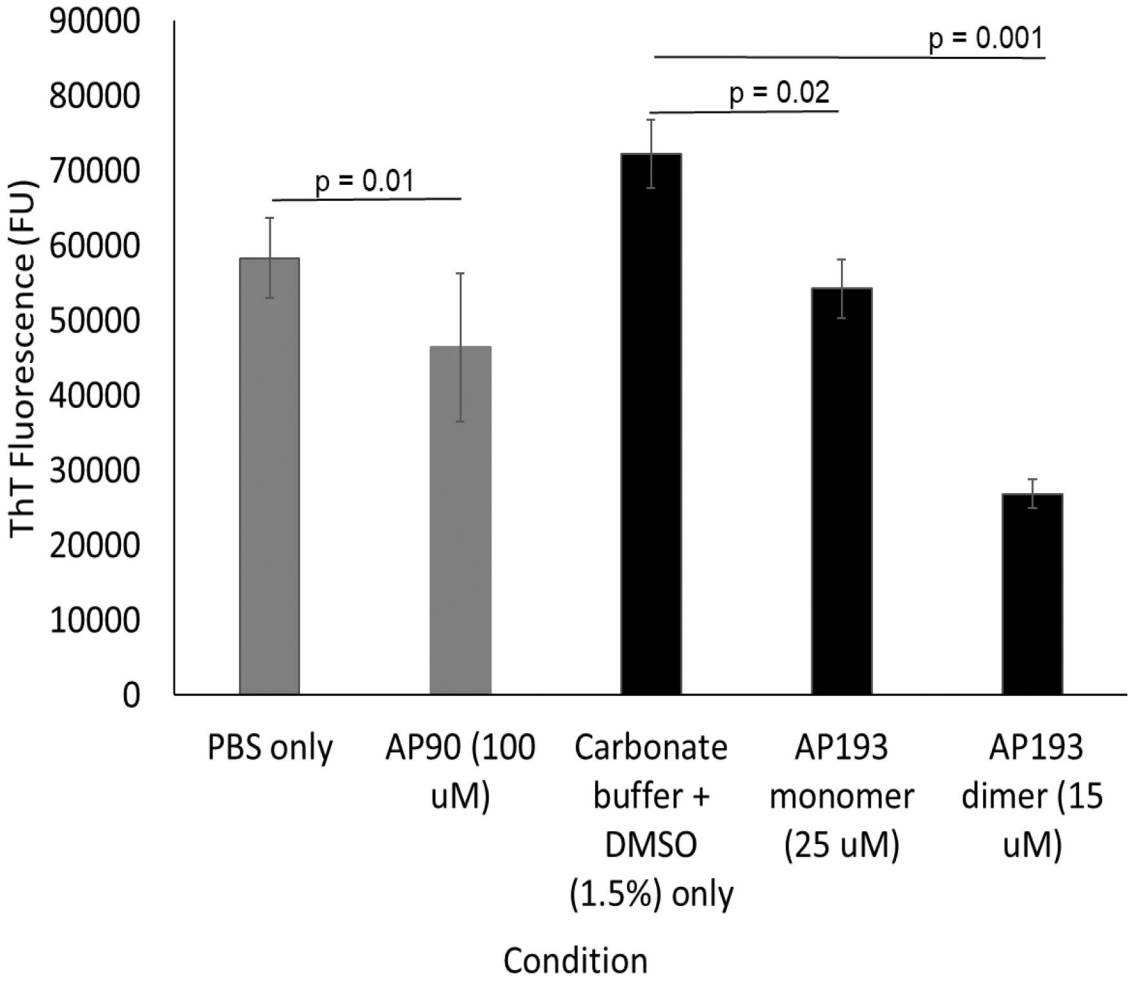

Figure 8.

α-sheet peptides added to *S. mutans* grown on hydroxyapatite ceramic particles led to significant decreases in ThT fluorescence. 100 μM AP90 reduced ThT fluorescence by 20%, whereas AP193 monomer and dimer in DMSO (1.5%) in carbonate buffer reduced ThT fluorescence by 23% and 63%, respectively at low concentrations of 25 μM and 15 μM.

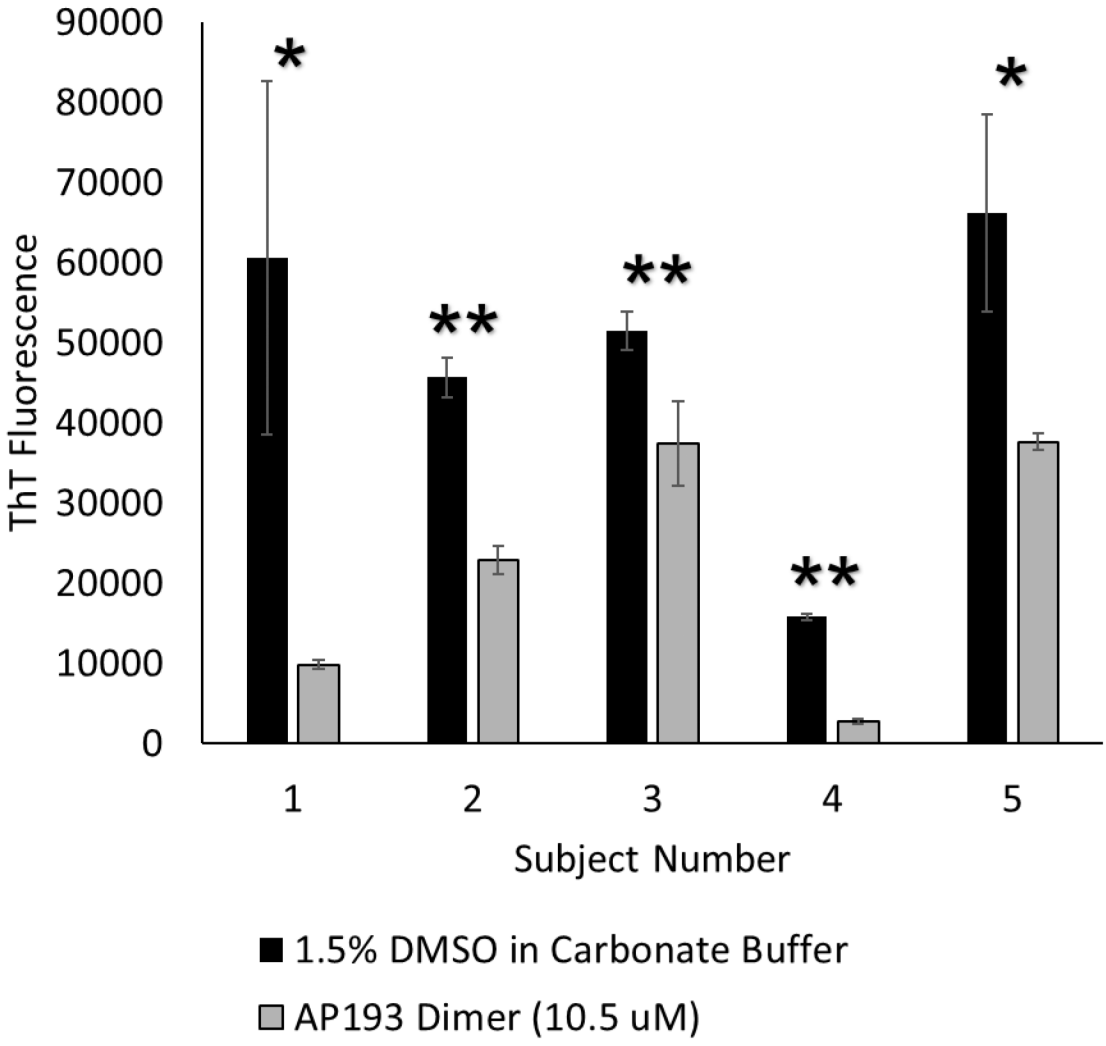

Figure 9.

Whole human saliva samples were obtained from donors, and grown on hydroxyapatite ceramic particles with solvent only, or with AP193 dimer at 10.5 μM. Addition of peptide to saliva from every donor led to significant decreases in ThT fluorescence of cells grown on the hydroxyapatite ceramic particles. The reduction in ThT fluorescence ranged from 27% (subject 3) to 83% (subject 1). (* = $p < 0.05$, ** = $p < 0.01$, compared to vehicle only)

Table 1.

Peptide used in this study and their secondary structures[a]

Peptide Name	Secondary Structure	Sequence
AP90	α-sheet	Ac-RGEmNISwMNEYSGWtMnLkMGR-NH2
AP193		Ac-RGEmNyFwMNEYYGWtMnCkMGR-NH2
AP407		Ac-RGEmNICwMNEYSGWcMnLkMGR-NH2
P411	β-sheet	SWTWEpNKWTWK-NH2
P1	Random coil	Ac-KLKpLLTSENTL-NH2

[a]D-amino acids are indicated by lower-case letters and the α-strand regions are shaded.